bioRxiv preprint doi: https://doi.org/10.1101/047589; this version posted April 8, 2016. The copyright holder for this preprint (which was not certified by peer review) is the author/funder, who has granted bioRxiv a license to display the preprint in perpetuity. It is made available under aCC-BY-NC-ND 4.0 International license.

Crossover in the dynamics of cell wall growth controls bacterial division times

Shiladitya Banerjee,[1] Klevin Lo,[1,2] Thomas Kuntz,[3] Matthew K. Daddysman,[2] Aaron R. Dinner,[1,2,3,*] and Norbert F. Scherer[1,2,3,*]

[1] *James Franck Institute, The University of Chicago, Chicago IL 60637*

[2] *Institute for Biophysical Dynamics, The University of Chicago, Chicago IL 60637*

[3] *Department of Chemistry, The University of Chicago, Chicago IL 60637*

Cell size is specific to each species and impacts their ability to function. While various phenomenological models for cell size regulation have been proposed, recent work in bacteria have demonstrated an *adder* mechanism, in which a cell increments its size by a constant amount between each division. However, the coupling between cell size, shape and constriction, remain poorly understood. Here, we investigate size control and the cell cycle dependence of bacterial growth, using multigenerational cell growth and shape data for single *Caulobacter crescentus* cells. Our analysis reveals a biphasic growth mechanism: a *timer* phase before constriction where the cell grows by a constant multiple of its initial size, followed by an *adder* phase during constriction. Synchronized cell wall labeling measurements reinforce this biphasic behavior: a crossover from uniform lateral growth to localized septal growth is observed. We quantitatively explain this *mixer mechanism* for size control using a mathematical model.

We recently introduced a technology that enables obtaining unprecedented amounts of precise quantitative information about the shapes of single bacteria as they grow and divide under non-crowding and controllable environmental conditions [1, 2]. Others have developed complementary methods [3–5]. These single-cell studies are generating great interest because they reveal unanticipated relationships between cell size and division control [5]. Recent work in bacteria that utilize these technologies revealed that a constant size increment between successive generations quantitatively describes the strategy for bacterial size maintenance in *E. coli* [3, 5, 6], *B. subtilis* [5], *C. crescentus* [4], and even in the yeast *S. cerevisiae* [7]. This phenomenological observation has been termed an *adder* model for cell size control. Competing models for size control include cell

* To whom correspondence may be addressed. Email: dinner@uchicago.edu or nfschere@uchicago.edu.

bioRxiv preprint doi: https://doi.org/10.1101/047589; this version posted April 8, 2016. The copyright holder for this preprint (which was not certified by peer review) is the author/funder, who has granted bioRxiv a license to display the preprint in perpetuity. It is made available under aCC-BY-NC-ND 4.0 International license.

division at a critical size (*sizer* model) [8] or at a constant interdivision time (*timer* model) [1]. Analysis of single-cell data show that cell size at division is positively correlated with the cell size at birth [1, 4, 5, 9, 10], thus precluding a sizer model. In addition, a negative correlation between initial cell size and interdivision times, as reported here and in refs [1, 4, 5, 10, 11], is inconsistent with the timer model. However, other studies have suggested mixed models of size control, with diverse combinations of sizer, timer and adder mechanisms [12–14]. The resolution of our data now allow us to revisit these issues with greater precision.

While cell size serves as an important determinant of growth, the bacterial cell cycle is composed of various coupled processes including cell wall constriction and DNA replication that have to be faithfully coordinated for cells to successfully divide [15]. This raises the question of what other cell cycle variables regulate growth and how the interplay between these different coupled variables can be understood quantitatively [16, 17]. Indeed, our recent analysis of cell shapes revealed how different cell shape variables are coupled through growth and division [2]. Our shape analysis further led to the development of a general physical theory for cell shape dynamics [18], which provides testable quantitative predictions for the interplay between cell shape, growth and division control.

Here we transcend our previous works by relating the mechanism of cell size control and cell wall growth to the timing of cell-wall constriction in *C. crescentus* cells. Our experimental data and analysis reveal that a *C. crescentus* cell grows by a constant multiple of its initial size prior to constriction (a *timer* mechanism), and adds a constant size during cell-wall constriction leading to the formation of daughter cell poles (an *adder* mechanism). We term this biphasic size regulation behavior a *mixer* mechanism for cell size control, and we find it to be operative over the range of physiologically relevant temperatures of the organism. Furthermore, by fluorescently labeling the cell walls of a synchronized population of *C. crescentus* cells and analyzing the resultant spatial profiles, we find a crossover in cell wall growth dynamics from uniform lateral growth to localized septal growth at the onset of cell wall constriction; that is, a crossover from a timer to an adder mechanism. This finding motivated our development of a mathematical model of the physical origin of cell size control.

RESULTS

We use a combination of microfluidics and phase-contrast microscopy for high-throughput, live-cell measurements of cell shape dynamics of single *C. crescentus* cells [1, 2, 19] (see Supplementary

bioRxiv preprint doi: https://doi.org/10.1101/047589; this version posted April 8, 2016. The copyright holder for this preprint (which was not certified by peer review) is the author/funder, who has granted bioRxiv a license to display the preprint in perpetuity. It is made available under aCC-BY-NC-ND 4.0 International license.

Methods). As a population of cells is controllably attached via a stalk and holdfast to the coverslip surface in the microfluidic channel, our measurements allow obtaining accurate and precise data of single cell shape and growth for >10000 generations for >250 cells under steady environmental conditions. From the splined cell contours of the acquired phase-contrast images (Fig. 1A), we determine various cell shape parameters, such as the length of the cell midline axis (l), the width of the cell, and also the radius of curvature of the midline. As reported previously, the length (l) increases exponentially with time constant $\langle\kappa\rangle^{-1} = 125 \pm 8$ min and a mean division time $\langle\tau\rangle = 73 \pm 7$ min at 31°C (in peptone-yeast extract medium), while the average width and the radius of curvature remains approximately constant [2]. Since measurements of the cell area behave the same as the length [1], we use the length of the midline axis of the cell, l, as a metric for cell size.

Mixer model of cell size control. We first analyzed the correlation between cell size at birth, $l(0)$, and the cell size at division, $l(\tau)$, since it reflects the intergenerational strategy for cell size control. While we previously considered only pure timer ($l(\tau) = al(0)$) and adder ($l(\tau) = l(0) + \delta$) models [1], here, consistent with [14], we find that the final cell size can best be described by a model that combines them: $l(\tau) = al(0) + \delta$, with a slope of $a = 1.25$ and an intercept $\delta = 1.39$ μm (Fig. 1B; Supplementary Information; Supplementary Figure 1). The value of the slope should be compared with 1.76, the multiple expected for a mean division ratio of $\simeq 0.54$ between the daughter cells. Since the cells grow at a constant exponential growth rate, κ, the non-zero positive value of the intercept δ implies negative feedback control of cell size [4–6, 10],

$$\tau = \kappa^{-1} \ln \left[a + \delta/l(0)\right] . \tag{1}$$

We find the interdivision times, τ, to be negatively correlated with the initial cell lengths (Eq. (3); Fig. 1C). In addition, as shown in Fig. 1D, the distribution of normalized cell cycle times, $\kappa\tau$, are also correlated with the initial lengths as shown by the conditional probability $P(\kappa\tau|l(0)/\langle l(0)\rangle)$ for various ranges of $l(0)/\langle l(0)\rangle$. These observations rule out a timer mechanism of cell size control where the division times would be uncorrelated with the initial lengths. Furthermore, Figures 1E and F show that the lengths added in each generation, $\Delta l = l(\tau) - l(0)$, are positively correlated with the initial cell lengths, which precludes an adder model for cell size control, in contrast to [4]. Our experiments suggest that *C. crescentus* cells behave as a *mixer*, with both timer and adder components. Furthermore, we find that this mixer mechanism is conserved in the temperature range 17°C-34°C (Supplementary Figures 2,3). Interestingly cells at 37°C behave as a perfect adder, which suggests that the adder result in [4] may be elicited by the conditions of that experi-

bioRxiv preprint doi: https://doi.org/10.1101/047589; this version posted April 8, 2016. The copyright holder for this preprint (which was not certified by peer review) is the author/funder, who has granted bioRxiv a license to display the preprint in perpetuity. It is made available under aCC-BY-NC-ND 4.0 International license.

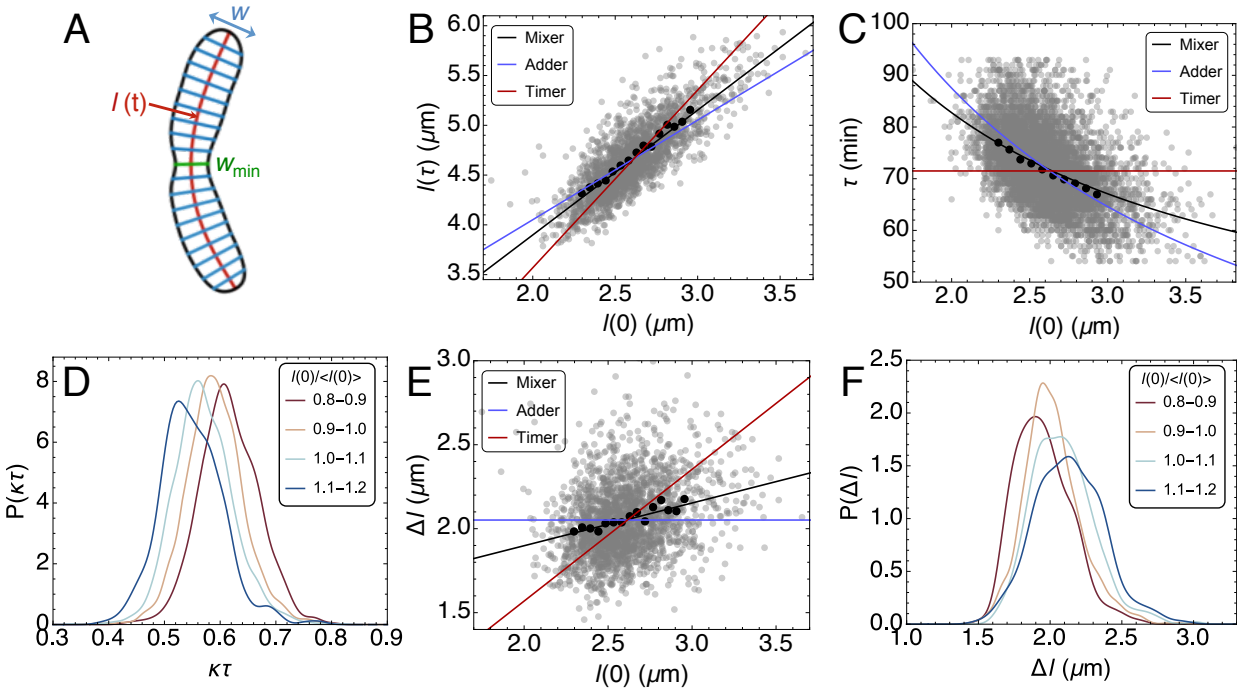

FIG. 1. **Cell size and division control in *C. crescentus* cells**. (A) A representative splined contour of a *C. crescentus* cell, illustrating the shape variables. (B) Cell size at division, $l(\tau)$, vs the cell size at birth, $l(0)$. The black solid line represents a least square linear fit to all single generation data given by the gray scatter cloud (mixer model). Corresponding fits by timer and adder models are given by red and blue lines, respectively. The solid circles represent mean data binned in $l(0)$. (C) The scatter plot of interdivision times, τ, vs the initial cell size, $l(0)$, exhibits a negative correlation. The black solid line is the prediction from our exponential growth and mixer model with no adjustable fitting parameters. Predictions from timer and adder models are shown by the red and blue lines. (D) The conditional probability density of normalized cell cycle time, $\kappa\tau$, given the mean rescaled initial length values, $P(\kappa\tau|l(0)/\langle l(0)\rangle)$, illustrating the negative feedback between τ and $l(0)$. The distributions were generated using a kernel density estimation [20]. (E) Size extension in each generation, Δl is correlated with the initial cell size. The mean trend is described by the linear relationship, $\Delta l = (a-1)l(0)+\delta$, which is the mixer model. (F) shows the conditional probability density of size extension Δl given the mean rescaled initial cell length, $P(\Delta l|l(0)/\langle l(0)\rangle)$.

ment. For *C. crescentus*, 37°C is the extreme upper limit for viable cell growth.

Crossover in cell wall growth dynamics. Since a mixer model implements a timer ($al(0)$) and an adder component (δ) serially, we conducted experiments to determine if we can visualize a crossover from timer to adder behavior in the cell cycle. We sought to examine the cell cycle dependence of peptidoglycan synthesis, by using a fluorescent construct of lectin wheat germ agglutinin (flWGA) that labels the cell wall of Gram-negative *C. crescentus* cells [21] (see Sup-

bioRxiv preprint doi: https://doi.org/10.1101/047589; this version posted April 8, 2016. The copyright holder for this preprint (which was not certified by peer review) is the author/funder, who has granted bioRxiv a license to display the preprint in perpetuity. It is made available under aCC-BY-NC-ND 4.0 International license.

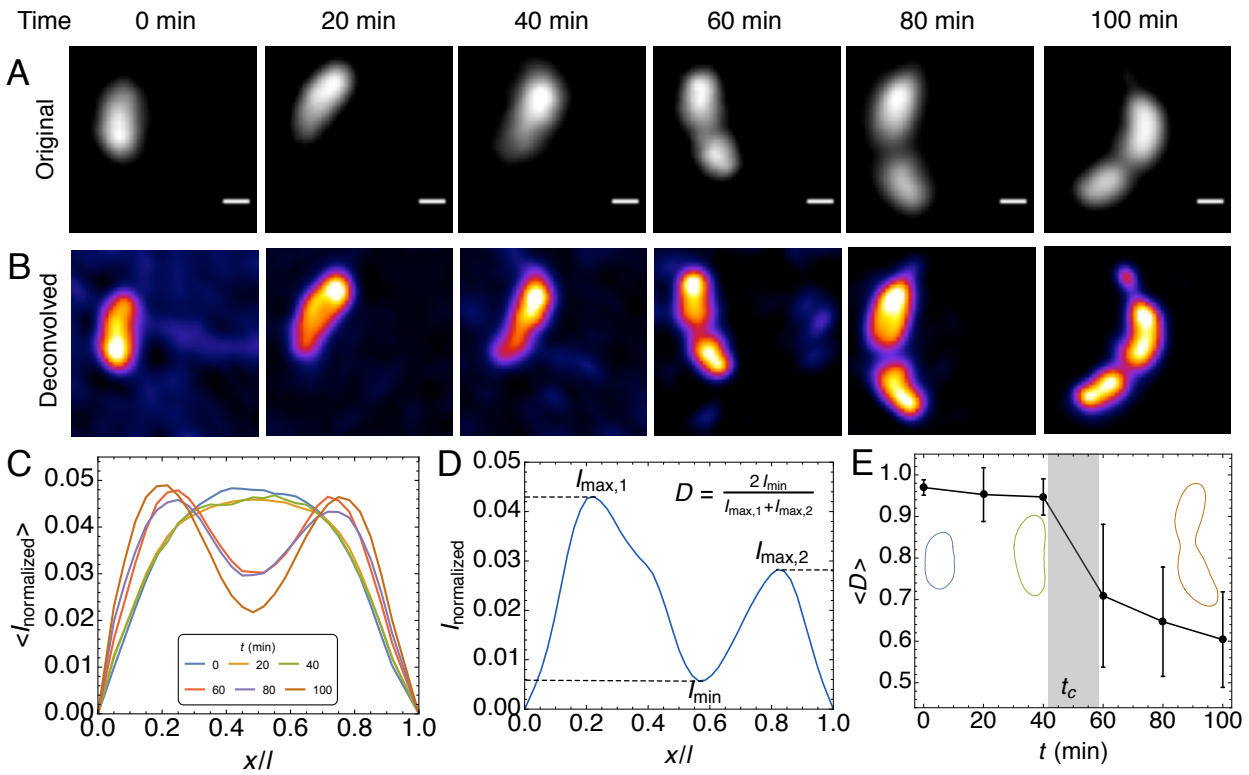

FIG. 2. **Crossover in cell wall growth dynamics at the onset of constriction**. (A) Confocal fluorescent images of *C. crescentus* cells labeled with fluorescent WGA taken after 0, 20, 40, 60, 80 and 100 min of growth in culture medium. The scale bars represent 0.5 μm. (B) Shows the same data but deconvoluted using the Huygens software package (see Supplementary Methods). The depletion of fluorescence reveals the underlying spatial pattern of growth, i.e. growth occurs where the fluorescence is minimized. (C) Ensemble averaged spatial distribution of normalized flWGA intensity along the centerline axis of the cell at t =0, 20, 40, 60, 80 and 100 min. The arc length along centerline, x, is normalized by the cell length, l. (D) A typical intensity profile is characterized by one minimum at the septum ($I_{\min}$) and two maxima near either pole ($I_{\max,1}$, $I_{\max,2}$). We define the index of uniformity of cell wall growth as, $D = 2I_{\min}/(I_{\max,1} + I_{\max,2})$. See Supplementary Information for more details. (E) Ensemble averaged dynamics of the growth uniformity index ($\langle D \rangle$) reveal a crossover from uniform growth ($\langle D \rangle \simeq 1$) to localized septal growth between 40 to 60 min (shaded area). Error bars indicate ± 1 standard deviation. The inset shows representative splined cell contours.

plementary Methods). Cells were initially synchronized to a uniform cell cycle phase by isolating the swarmer from the stalked cells and were subsequently incubated in flWGA [22]. The cells were then left to grow in media without flWGA and were isolated at specific time points along the cell cycle. The isolated cells were then immediately fixed to preserve the cell-wall growth patterning at a given phase (Fig. 2A). Fig. 2A shows that the fluorescence intensity is spatially

bioRxiv preprint doi: https://doi.org/10.1101/047589; this version posted April 8, 2016. The copyright holder for this preprint (which was not certified by peer review) is the author/funder, who has granted bioRxiv a license to display the preprint in perpetuity. It is made available under aCC-BY-NC-ND 4.0 International license.

uniform prior to constriction (i.e., for samples at $t < 40$ min), but the flWGA intensity patterns exhibit a pronounced minimum at the septum where the cell-wall is invaginated ($t > 60$ min). Fig. 2B presents deconvolution processed images obtained using commercial software (Huygens). The deconvoluted single cell images more clearly show the diminished flWGA label in the septal region. Moreover, the 100 min image even hints at secondary invaginations in a predivisional cell, consistent with our previous report on intergenerational continuity [2]. Fig. 2C shows the ensemble averaged normalized intensity profiles along the centerline axis of the cell at different time points. The spatial distribution of flWGA intensity suggests that growth is spatially uniform for $t < 40$ min and new cell-wall material is primarily synthesized at the invaginations for $t > 40$ min. This septal mode of cell wall growth has been reported earlier with D-amino acid labeling of the cell wall [23]. To quantify the spatial uniformity of cell-wall deposition for each cell in the ensemble ($\sim$135 cells) we introduce a *growth uniformity index*, D, given by the ratio of the intensity at the site of the septum ($I_{\min}$) to the mean of the maximum intensities ($I_{\max,1,2}$) on the stalked and swarmer sides of that site (Fig. 2D; Supplementary Information). The ensemble averaged growth uniformity index, $\langle D \rangle$, is close to unity for $t < 40$ min (since $I_{\min} \simeq I_{\max,1,2}$), indicating spatially uniform growth (Fig. 2E). For $t > 60$ min, $\langle D \rangle$ dropped sharply to lower values, suggesting that cell wall growth is localized to the septum and is thus coupled to cell wall constriction.

Timer phase prior to cell wall constriction. To relate this observed crossover in cell wall growth to the dynamics of other cell cycle variables, we examined our single cell shape data [2]. We find that the constriction dynamics in individual generations exhibit pronounced biphasic behavior, with an initial period of slow constriction followed by a phase of fast constriction (Figure 3A). We determine the crossover time, t_c, by fitting exponential curves to the initial and the later phases of decay in $w_{\min}(t)$. We define the onset of constriction by t_c, which has a mean value $t_c = 41.1 \pm 3.2$ min at 31°C (Fig. 3A, inset). This crossover dynamic is observed in the analogous data obtained at other temperatures of the medium; we find that t_c increases in proportion to τ as the temperature is decreased (Supplementary Figures 4, 5). As shown in Figs. 3B and C, the conditional distributions of the normalized crossover times, $\kappa t_c = \ln[l(t_c)/l(0)]$, collapse to a single curve for various values of $l(0)/\langle l(0) \rangle$ and $\tau/\langle \tau \rangle$. These observations suggest that the relative size extension, given by $l(t_c)/l(0)$, is independent of initial cell length and interdivision times. Indeed our data show that κt_c is uncorrelated with the initial cell size (Fig. 3D, red cloud), whereas the cell length at $t = t_c$ is a constant multiple of the initial length, $l(t_c) \simeq 1.36\ l(0)$ (Fig. 3E, red cloud). By analyzing our shape data at other temperatures we find that $l(t_c)$ remains a constant multiple of $l(0)$ (Sup-

bioRxiv preprint doi: https://doi.org/10.1101/047589; this version posted April 8, 2016. The copyright holder for this preprint (which was not certified by peer review) is the author/funder, who has granted bioRxiv a license to display the preprint in perpetuity. It is made available under aCC-BY-NC-ND 4.0 International license.

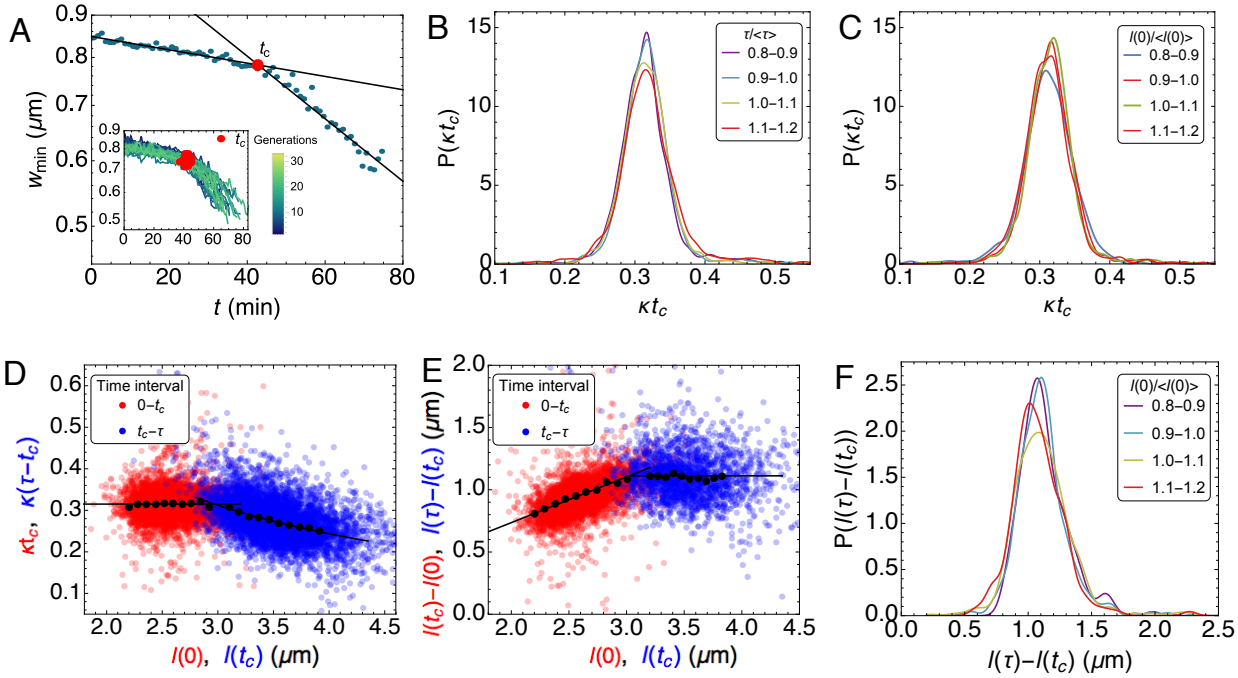

FIG. 3. **Crossover from timer to adder-like behavior at the onset of cell wall constriction.** (A) Semi-log plot of the time-dependence of $w_{\min}$ in a typical generation shows two phases of constriction, a slow initial phase followed by a fast constriction phase. We determine t_c by the intersection of the least square exponential fits to the initial and latter portions of the cell cycle. Inset: Dynamics of $w_{\min}$ across generations of a typical cell. Locations of t_c are marked by red solid circles. (B) The conditional probability density of normalized crossover time, κt_c, given the mean rescaled division times, $P(\kappa t_c|\tau/\langle\tau\rangle)$, showing the independence of κt_c and τ. (C) The conditional probability density of the normalized crossover time, κt_c, given the mean rescaled initial length values, $P(\kappa t_c|l(0)/\langle l(0)\rangle)$, showing the independence of κt_c and $l(0)$. (D) Lack of correlation between κt_c and $l(0)$ (red scatter) and negative feedback between $\kappa(\tau - t_c)$ and $l(0)$ (blue scatter). Black curves represent pure timer [$l(t_c) = 1.36l(0)$; red scatter] and pure adder [$l(\tau) = l(t_c) + 1.1$; blue scatter] fits in the two phases. The solid circles represent mean data binned in $l(0)$. (E) Positive correlation between the added size before constriction, $\delta' = l(t_c) - l(0)$ and $l(0)$ (red scatter). Added size for $t > t_c$, δ' is uncorrelated with $l(t_c)$ (blue scatter) supporting an adder model during the constriction phase. (F) The conditional probability density of the added cell size, δ', given the mean rescaled initial lengths, $l(0)/\langle l(0)\rangle$. The collapse of the distributions indicates the independence of δ' and $l(0)$.

plementary Figure 6A). As expected from a pure timer mechanism, κt_c remains uncorrelated with $l(0)$ at all temperatures with a constant mean value $\simeq 0.33$ (Supplementary Figure 6B). Taken together our data reveal a timer mechanism prior to the onset of cell wall constriction, i.e. prior to t_c.

bioRxiv preprint doi: https://doi.org/10.1101/047589; this version posted April 8, 2016. The copyright holder for this preprint (which was not certified by peer review) is the author/funder, who has granted bioRxiv a license to display the preprint in perpetuity. It is made available under aCC-BY-NC-ND 4.0 International license.

Adder phase during cell wall constriction. While the time to the onset of cell wall constriction is uncorrelated with cell size, the added size in the constriction phase, $\delta' = l(\tau) - l(t_c)$, also showed no correlation with $l(t_c)$ (Fig. 3E, blue cloud). This suggests an *adder* mechanism of cell size control for $t_c < t < \tau$, such that the distribution of the added size is independent of the initial cell length. This adder behavior is indeed confirmed by the collapse of the conditional distributions of the added size $P(\delta'|l(0)/\langle l(0)\rangle)$ to a single curve (Fig. 3F). Furthermore, the time to divide since t_c shows negative correlation with $l(t_c)$ (Fig. 3D, blue cloud). This negative correlation is supported by a model of constant size extension or an *adder* during the constriction phase, $\tau = t_c + \kappa^{-1} \log\left[1 + \langle\delta'\rangle/l(t_c)\right]$ with $\langle\delta'\rangle = 1.1$ μm (Fig. 3D, solid line). Furthermore, we find that the adder phase post constriction is conserved for all temperatures with a constant mean added size 1.1 μm (Supplementary Figures 6 C,D). Since constricting cells primarily grow from the septum (Fig. 2), the added size in the constriction phase is expected to be proportional to the width of the septal plane. Consistent with the model of septal growth, we find that δ' is positively correlated with $w_{\min}(t_c)$ (Supplementary Fig. 7A).

Model for constriction driven by septal growth describes the crossover dynamics. To examine whether septal cell wall synthesis in exponentially elongating cells (Fig. 2) can reproduce the observed crossover dynamics of constriction (Fig. 3), we consider a quantitative model for cell wall constriction driven by septal growth that we recently reported [18]. We assume that the shape of the constriction zone is given by two intersecting hemispherical segments with diameter w, and constriction proceeds by completing the missing parts of the hemispheres while maintaining the curvature of the preformed spherical segments. The total surface area of the septum is given by $S(t) = \pi w l_s(t)$, where $l_s(t)$ is the total length of the hemispherical segments (Fig. 4A). Since constriction proceeds concomitantly with longitudinal growth [2], exponential growth of septal surface area implies:

$$\frac{dl_s}{dt} = \kappa(l_s + l_0) \ , \tag{2}$$

where l_0 is the length of the septum synthesized following the initiation of constriction, which we determine by fitting our model to the data for $w_{\min}(t)$. The solution to Eq. (2) can then be used to derive the time-dependence of $w_{\min}(t) = \sqrt{w^2 - l_s(t)^2}$. Using the initial condition, $l_s(0) = 0$, we derive a simple relation

$$w_{\min}(t)/w_{\min}(0) = \sqrt{1 - \left(l_0/w_{\min}(0)\right)^2 \left(e^{\kappa t} - 1\right)^2} \ ,$$

bioRxiv preprint doi: https://doi.org/10.1101/047589; this version posted April 8, 2016. The copyright holder for this preprint (which was not certified by peer review) is the author/funder, who has granted bioRxiv a license to display the preprint in perpetuity. It is made available under aCC-BY-NC-ND 4.0 International license.

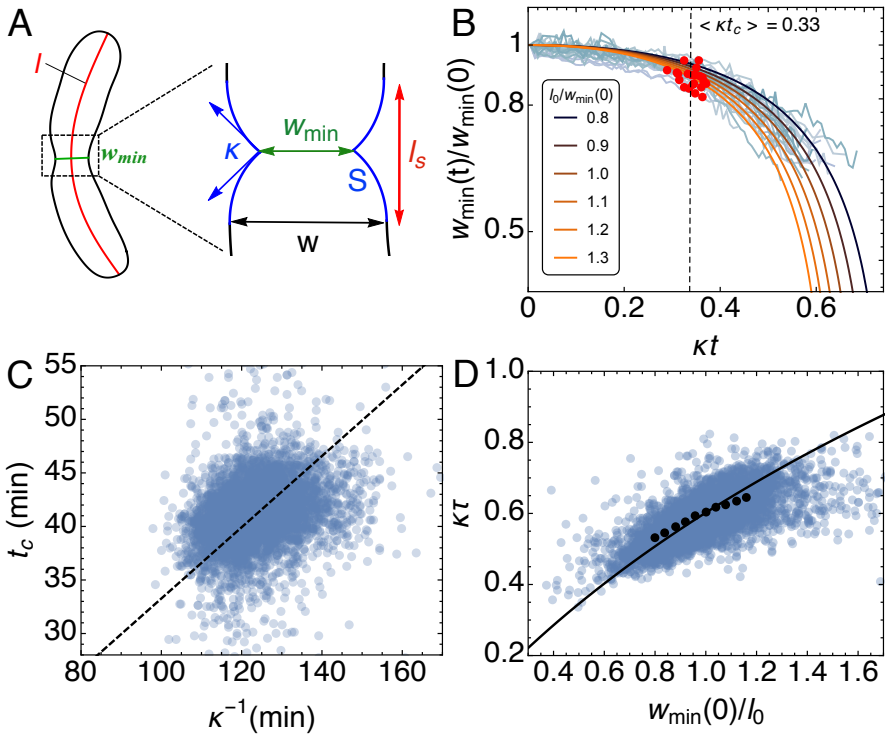

FIG. 4. **Septal growth model predicts the onset of cell wall constriction and interdivision times**. (A) A representative splined contour of a *C. crescentus* cell, illustrating the shape parameters, l (red) and $w_{\min}$ (green). The dashed region represents the constriction zone, where S is the surface area of the septal cell-wall (blue) synthesized after constriction. (B) Dynamics of the width of the pinch-off plane (normalized by $w_{\min}(0)$), with time normalized by κ^{-1}. Predictions of the septal growth model are shown by solid curves at various values of the dimensionless parameter, $l_0/w_{\min}(0)$, which controls the interdivision times but not the crossover (dashed line). Experimental data for different generations of a representative cell are shown in light blue with the locations of the crossover marked by solid red circles. (C) Positive correlation between t_c and κ^{-1}. The dashed line represents the predicted crossover curve $t_c = 0.33\kappa^{-1}$. (D) Normalized interdivision times ($\kappa\tau$) vs the normalized initial width of the pinch-off plane (binned data in solid circles; model prediction, Eq. (3), in solid curve).

between the rescaled width and the rescaled time variable (κt). The dynamics of constriction is then solely controlled by the dimensionless parameter $l_0/w_{\min}(0)$. As shown in Fig. 4B, the time to the onset of fast constriction is insensitive to variations in $l_0/w_{\min}(0)$, and the model prediction for the crossover time is in excellent agreement with the mean crossover time in our experimental data ($\langle \kappa t_c \rangle = 0.33$, Fig. 4B). This implies that t_c is regulated by the longitudinal growth rate κ, which is consistent with the observed positive correlation between t_c and κ^{-1} (Fig. 4C).

Another prediction of the constriction model is that the interdivision times increase with increasing $w_{\min}(0)/l_0$, because the wider cells require more material to close the septum. Based on

bioRxiv preprint doi: https://doi.org/10.1101/047589; this version posted April 8, 2016. The copyright holder for this preprint (which was not certified by peer review) is the author/funder, who has granted bioRxiv a license to display the preprint in perpetuity. It is made available under aCC-BY-NC-ND 4.0 International license.

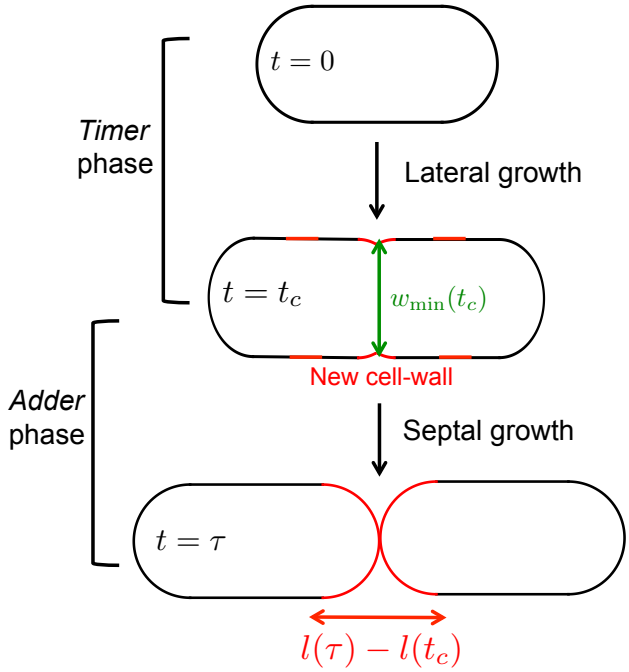

FIG. 5. **Mixer mechanism for cell wall growth.** A schematic of the mixer model for spatiotemporal coordination of cell wall growth in *C. crescentus* cells. Growth is spatially uniform for $t < t_c$ when cell wall deposition occurs laterally along the entire cell length except the poles. For $t > t_c$, cell wall growth is dominated by septal cell wall synthesis that leads to constant size extension determined by the surface area of the new poles.

our model, we predict a simple relation between the interdivision times and the initial width of the constriction plane,

$$\tau = \kappa^{-1} \log \left(1 + \frac{\Delta w_{\min}}{l_0} \right) , \tag{3}$$

where, $\Delta w_{\min} = \sqrt{w_{\min}(0)^2 - w_{\min}(\tau)^2}$. Thus, the interdivision time is predicted to be larger for cells with larger septum width, $\Delta w_{\min}$. We find a positive correlation in our data between $\kappa\tau$ and $w_{\min}(0)/l_0$, and the mean trend in our data is in good quantitative agreement with our model with no fitting parameters (Fig. 4D). Furthermore, Eqs. (1) and (3) together imply a negative correlation between initial septal width, $w_{\min}(0)$, and the cell size at division, $l(\tau)$, which is in quantitative agreement with our data (Supplementary Figure 7B).

In summary, the septal growth model allows us to derive two key conclusions, supported by our data. First, the time to the onset of constriction (t_c) is controlled by the growth rate (κ). Second, the interdivision times are larger for cells with larger initial septal width.

bioRxiv preprint doi: https://doi.org/10.1101/047589; this version posted April 8, 2016. The copyright holder for this preprint (which was not certified by peer review) is the author/funder, who has granted bioRxiv a license to display the preprint in perpetuity. It is made available under aCC-BY-NC-ND 4.0 International license.

DISCUSSION

The adder phase of cell-wall growth ($t > t_c$) coupled with relative size thresholding prior to constriction ($t < t_c$) comprise a biphasic growth model for *C. crescentus* cells. This mechanism is illustrated using the schematic in Fig. 5. Newborn cells exhibit lateral elongation with uniform patterning of cell wall synthesis prior to constriction ($t < t_c$). Cells begin their constriction phase (at $t = t_c$) at a constant critical multiple of their initial sizes. During the constriction phase, $t > t_c$, cells primarily add new cell wall material at the septum. This phase of growth is characterized by a constant cell size extension. The length added after $t > t_c$ originates primarily from the surface area of the daughter cell poles. Taken together, the crossover from uniform cell wall growth to localized septal growth provides a physical basis for a *mixer model* of cell size control, $l(\tau) = e^{\kappa t_c} l(0) + \delta'$. Like the adder model, the mixer model automatically ensures cell size homeostasis: with each division, the cell length regresses to the ensemble average [14, 24], $\delta r/(1 - ar)$, where $r \simeq 0.54$ is the mean ratio of the daughter to the mother cell size (length). It is interesting to consider why *E. coli* exhibits a pure adder behavior while *C. crescentus* exhibits a mixer behavior. One notable difference between the species is that *E. coli* can initiate multiple rounds of DNA replication per cell cycle while *C. crescentus* has a strict one-to-one correspondence between these processes.

While the molecular mechanism for the control of the onset of cell wall constriction is unknown, it is likely that t_c is determined by the time of assembly of FtsZ protofilaments that builds a polymeric structure called the Z-ring at the plane of cell division. The Z-ring acts as a scaffold for the assembly of the divisome, directing the synthesis of new cell-wall material at the septum [25]. Previous studies have reported a metabolic sensor in bacteria that regulates cell size control by inhibiting the assembly of the Z-ring [26]. The upstream regulator of Z-ring assembly is the ATPase MipZ, which directly interacts with FtsZ and inhibits its polymerization at the poles [27, 28]. Cells lacking MipZ become filamentous and are unable to divide [27]. This suggests that the onset of the adder phase of cell-wall growth is controlled by the time for localization of MipZ proteins at the cell poles. While cell cycle checkpoints have so far not been established in bacteria, unlike eukaryotic cells, it is likely that MipZ gradients can serve as an internal sensor of cell size similar to the Pom1 gradient model of length sensing in fission yeast in the G2/M phase [29]. This insight provides a prediction for further investigation into the molecular candidates regulating cell size and division control in bacteria.

bioRxiv preprint doi: https://doi.org/10.1101/047589; this version posted April 8, 2016. The copyright holder for this preprint (which was not certified by peer review) is the author/funder, who has granted bioRxiv a license to display the preprint in perpetuity. It is made available under aCC-BY-NC-ND 4.0 International license.

REFERENCES

[1] Iyer-Biswas, S. *et al.* Scaling laws governing stochastic growth and division of single bacterial cells. *Proceedings of the National Academy of Sciences* **111**, 15912–15917 (2014).

[2] Wright, C. S. *et al.* Intergenerational continuity of cell shape dynamics in caulobacter crescentus. *Scientific Reports* **5**, 9155 (2015).

[3] Wang, P. *et al.* Robust growth of escherichia coli. *Current Biology* **20**, 1099–1103 (2010).

[4] Campos, M. *et al.* A constant size extension drives bacterial cell size homeostasis. *Cell* **159**, 1433–1446 (2014).

[5] Taheri-Araghi, S. *et al.* Cell-size control and homeostasis in bacteria. *Current Biology* **25**, 385–391 (2015).

[6] Amir, A. Cell size regulation in bacteria. *Physical Review Letters* **112**, 208102 (2014).

[7] Soifer, I., Robert, L. & Amir, A. Single-cell analysis of growth in budding yeast and bacteria reveals a common size regulation strategy. *Current Biology* (2016).

[8] Donachie, W. Relationship between cell size and time of initiation of dna replication. *Nature* **219**, 1077–1079 (1968).

[9] Koppes, L., Meyer, M., Oonk, H., De Jong, M. & Nanninga, N. Correlation between size and age at different events in the cell division cycle of escherichia coli. *Journal of Bacteriology* **143**, 1241–1252 (1980).

[10] Osella, M., Nugent, E. & Lagomarsino, M. C. Concerted control of escherichia coli cell division. *Proceedings of the National Academy of Sciences* **111**, 3431–3435 (2014).

[11] Tanouchi, Y. *et al.* A noisy linear map underlies oscillations in cell size and gene expression in bacteria. *Nature* **523**, 357–360 (2015).

[12] Donachie, W., Begg, K. & Vicente, M. Cell length, cell growth and cell division. *Nature* **264**, 328–333 (1976).

[13] Kubitschek, H. Bilinear cell growth of escherichia coli. *Journal of Bacteriology* **148**, 730–733 (1981).

[14] Jun, S. & Taheri-Araghi, S. Cell-size maintenance: universal strategy revealed. *Trends in Microbiology* **23**, 4–6 (2015).

[15] Wang, J. D. & Levin, P. A. Metabolism, cell growth and the bacterial cell cycle. *Nature Reviews Microbiology* **7**, 822–827 (2009).

[16] Mitchison, J. M. *The biology of the cell cycle* (CUP Archive, 1971).

[17] Marshall, W. F. *et al.* What determines cell size? *BMC Biology* **10**, 101 (2012).

[18] Banerjee, S., Scherer, N. F. & Dinner, A. R. Shape dynamics of growing cell walls. *Soft Matter* **12**, 3442–3450 (2016). URL `http://dx.doi.org/10.1039/C5SM02991K`.

[19] Lin, Y., Li, Y., Crosson, S., Dinner, A. R. & Scherer, N. F. Phase resetting reveals network dynamics

bioRxiv preprint doi: https://doi.org/10.1101/047589; this version posted April 8, 2016. The copyright holder for this preprint (which was not certified by peer review) is the author/funder, who has granted bioRxiv a license to display the preprint in perpetuity. It is made available under aCC-BY-NC-ND 4.0 International license.

underlying a bacterial cell cycle. *PLoS Comput Biol* **8**, e1002778 (2012).

[20] Silverman, B. W. *Density estimation for statistics and data analysis*, vol. 26 (CRC press, 1986).

[21] Ursell, T. S. *et al.* Rod-like bacterial shape is maintained by feedback between cell curvature and cytoskeletal localization. *Proceedings of the National Academy of Sciences* **111**, E1025–E1034 (2014).

[22] Marks, M. E. *et al.* The genetic basis of laboratory adaptation in caulobacter crescentus. *Journal of Bacteriology* **192**, 3678–3688 (2010).

[23] Aaron, M. *et al.* The tubulin homologue ftsz contributes to cell elongation by guiding cell wall precursor synthesis in caulobacter crescentus. *Molecular Microbiology* **64**, 938–952 (2007).

[24] Voorn, W., Koppes, L. & Grover, N. Mathematics of cell division in escherichia coli. *Curr. Top. Mol. Genet* **1**, 187–194 (1993).

[25] Divakaruni, A. V., Baida, C., White, C. L. & Gober, J. W. The cell shape proteins mreb and mrec control cell morphogenesis by positioning cell wall synthetic complexes. *Molecular Microbiology* **66**, 174–188 (2007).

[26] Weart, R. B. *et al.* A metabolic sensor governing cell size in bacteria. *Cell* **130**, 335–347 (2007).

[27] Thanbichler, M. & Shapiro, L. Mipz, a spatial regulator coordinating chromosome segregation with cell division in caulobacter. *Cell* **126**, 147–162 (2006).

[28] Goley, E. D., Iniesta, A. A. & Shapiro, L. Cell cycle regulation in caulobacter: location, location, location. *Journal of Cell Science* **120**, 3501–3507 (2007).

[29] Moseley, J. B., Mayeux, A., Paoletti, A. & Nurse, P. A spatial gradient coordinates cell size and mitotic entry in fission yeast. *Nature* **459**, 857–860 (2009).

ACKNOWLEDGEMENTS

We thank Charles Wright and Srividya Iyer-Biswas for measurements and shape analysis of *C. crescentus* single cell data [1, 2]. We thank Alan Selawa for performing the deconvolution analysis of the fluorescently labelled cell images shown in Fig. 2. We gratefully acknowledge funding from the NSF Physics of Living Systems (NSF PHY-1305542), the NSF Materials Research Science and Engineering Center (MRSEC) at the University of Chicago (NSF DMR-0828854), the W. M. Keck Foundation and the Graduate Program in Biophysical Sciences at the University of Chicago (T32 EB009412/EB/NIBIB NIH HHS/United States). We thank Sean Crosson and Aretha Fiebig for contributing reagents, materials and helpful discussions.

AUTHOR CONTRIBUTIONS

S.B., K.L., A.R.D. and N.F.S. designed research; S.B., K.L., M.D. and T.K. performed research; S.B., K.L., A.R.D. and N.F.S. wrote the manuscript.

bioRxiv preprint doi: https://doi.org/10.1101/047589; this version posted April 8, 2016. The copyright holder for this preprint (which was not certified by peer review) is the author/funder, who has granted bioRxiv a license to display the preprint in perpetuity. It is made available under aCC-BY-NC-ND 4.0 International license.

COMPETING FINANCIAL INTERESTS

The authors declare no competing financial interests.